



Lawrence Berkeley Laboratory

UNIVERSITY OF CALIFORNIA

RECEIVED
LAWRENCE
BERKELEY LABORATORY

APR 5 1982

LIBRARY AND
DOCUMENTS SECTION

Submitted to Nuclear Physics A

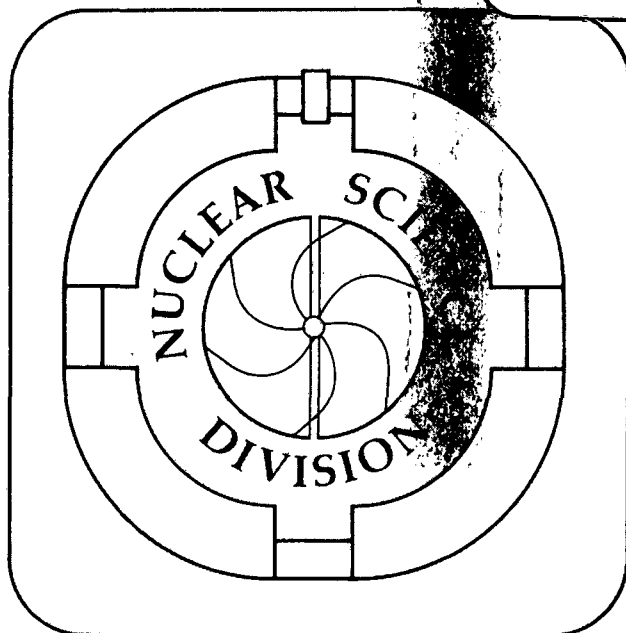
KINEMATICAL ANALYSIS OF THE EXPERIMENTAL DATA ON
NUCLEUS-NUCLEUS COLLISIONS AT 800 MeV/NUCLEON

V.I. Manko and S. Nagamiya

February 1982

TWO-WEEK LOAN COPY

*This is a Library Circulating Copy
which may be borrowed for two weeks.
For a personal retention copy, call
Tech. Info. Division, Ext. 6782*



LBL-14032
c.2

DISCLAIMER

This document was prepared as an account of work sponsored by the United States Government. While this document is believed to contain correct information, neither the United States Government nor any agency thereof, nor the Regents of the University of California, nor any of their employees, makes any warranty, express or implied, or assumes any legal responsibility for the accuracy, completeness, or usefulness of any information, apparatus, product, or process disclosed, or represents that its use would not infringe privately owned rights. Reference herein to any specific commercial product, process, or service by its trade name, trademark, manufacturer, or otherwise, does not necessarily constitute or imply its endorsement, recommendation, or favoring by the United States Government or any agency thereof, or the Regents of the University of California. The views and opinions of authors expressed herein do not necessarily state or reflect those of the United States Government or any agency thereof or the Regents of the University of California.

**KINEMATICAL ANALYSIS OF THE EXPERIMENTAL DATA
ON NUCLEUS-NUCLEUS COLLISIONS AT 800 MeV/ nucleon**

V. I. MANKO

I. V. Kurchatov Institute of the Atomic Energy, Moskow, U.S.S.R.

and

S. NAGAMIYA

Nuclear Science Division, Lawrence Berkeley Laboratory,
University of California, Berkeley, California 94720, U.S.A.

and

Department of Physics, Faculty of Science, University of Tokyo,
Hongo, Bunkyo-ku, Tokyo, Japan.

Abstract:

A purely empirical kinematical analysis of the existing data on nucleus-nucleus collisions at the beam energy of 800 MeV/nucleon is presented. We searched for a moving frame (frames) in which particles are emitted symmetrically about 90° , and found that three frames might exist in the mid-rapidity region. For nearly equal-mass collisions the rapidities of these frames are 0.22, 0.62 and 1.02. Emission of nuclear fragments in each frame has been studied. The cross section is factorized as a product of two Gaussian-type distributions, one which involves only p_T and the other which involves only p_L , where p_L is the longitudinal momentum measured in that frame. The present result is compared with the participant-spectator model. We propose two new sources which lie close to the projectile and target rapidities but have different natures from the spectator.

1. Introduction

During the last few years both experimental and theoretical studies of nucleus-nucleus collisions at high energies have made rapid progress¹⁾. A large number of experimental data have been reported, and several theoretical models have been proposed as well. Most of the theoretical models, however, succeed in reproducing certain aspects of the data on the one hand, whereas on the other hand they fail in reproducing others. This is not surprising, since the theoretical model is based on a simplification of the idea, whereas the actual data include various complex processes. Under such circumstances it may be worthwhile to analyze the existing data from a purely empirical method. The purpose of this paper is to report our recent empirical analysis of the existing data on various nucleus-nucleus collisions at 800 MeV/nucleon reported in refs.^{2,3)}.

Our approach is as follows: We first ask if there is a certain moving frame (or frames) in which fragments are emitted symmetrically about 90°. Once we find such a frame, we then ask how light nuclear fragments are emitted from it. Finally, we ask the meaning of this frame, namely, whether it indicates the existence of a certain source such as the fireball or it simply reflects the kinematical aspects alone. In particular, our present analysis is compared with the traditional participant-spectator model⁴⁻⁷⁾.

2. Search for Frames and the Fragment Spectra in Them

2.1. KINEMATICAL VARIABLES

In order to search for a moving frame (or frames) it is convenient to use a Lorentz-invariant cross section defined by

$$\sigma_{inv} = E \frac{d^3\sigma}{d^3p} \quad (1)$$

We also use relativistically invariant kinematical variables to describe the phase-space domain into which particles are emitted. The rapidity (y), which is the Lorentz-invariant longitudinal velocity, is defined by

$$y = \frac{1}{2} \ln \frac{E + p_L c}{E - p_L c} = \tanh^{-1}(p_L c / E). \quad (2)$$

The advantage of using y is that a longitudinal boost of the velocity v_0 along the beam direction simply adds a constant $y_0 (= \tanh^{-1}(v_0/c))$ to y . For example, if a certain c.m. frame is moving along the beam direction at a rapidity y_0 , then the particle rapidity as viewed in the laboratory frame (y^{Lab}) is related to the particle rapidity as viewed in this c.m. frame ($y^{c.m.}$) by

$$y^{Lab} = y^{c.m.} + y_0. \quad (3)$$

On the other hand, the Lorentz-invariant transverse velocity is given by

$$x = p_T / mc. \quad (4)$$

Using these two variables, x and y , the invariant cross section of Eq. (1) is now expressed as

$$\sigma_{inv} = \frac{1}{\pi m^2 c^2} \frac{d^2 \sigma}{dy dx^2}. \quad (5)$$

For example, a Boltzmann type fragment distribution in the nucleon-nucleon c.m. frame at 800 MeV/nucleon beam energy is shown in Fig. 1. There, invariant cross sections are plotted as a function of y for various values of x . Each curve has a maximum at $y = y_0 = 0.62$, where y_0 indicates the rapidity of this c.m. frame. In general, if particles are emitted symmetrically about 90° in a certain frame whose rapidity is y_0 , then the cross section reaches its maximum at $y = y_0$. By using such a feature we search for a moving frame (or frames) in the plot of invariant cross sections as a function of y .

2.2. NEARLY EQUAL-MASS COLLISIONS

We first consider the case of nearly equal-mass collisions, such as Ar + KCl and Ne + NaF. Shown in Fig. 2 are the observed cross sections, σ_{inv} , for p, d, t, and ^3He plotted as a function of y for various values of x . We immediately notice the following features:

- (a) For proton emission, especially at large values of x , the cross section peaks at $y_0 \approx 0.62$. This value corresponds to the c.m. frame of the whole system of projectile plus target.
- (b) For deuteron, triton and ^3He emissions, especially at small values of x , cross sections have two peaks. The value of y_0 for the first peak is about 0.22. The second peak is not clear from the data, but since the equal-mass collision should be symmetric with respect to the c.m. frame of the whole system, the value of y_0 for the second peak must be about $y_P - 0.22 \approx 1.02$, where y_P is the projectile rapidity. Therefore, we have three frames at $y_c \approx 0.22, 0.62$, and 1.02 . Hereafter we refer them as "slow", "moderate", and "fast" frames.

2.2.1. Particle Emission in 'Moderate' Frame

We now study particle spectra in each frame. As seen from Fig. 2, the proton emission for large values of x (≥ 0.5) is predominantly in the "moderate" frame. If we plot σ_{inv} at $y = y_0 \approx 0.62$ as a function of the transverse energy,

$$E_T / mc^2 = \sqrt{x^2 + 1} - 1, \quad (6)$$

then the data show a "shoulder-arm" type spectrum shape, as shown in Fig. 3 (left). This fact was already pointed out in ref.²⁾. Therefore, the proton emission is not a Boltzmann type. On the other hand, if we plot the same data as a function of x^2 , then they fall on a straight line, as shown in Fig. 3 (right). It implies that σ_{inv} at $y = y_0$ is expressed as

$$\sigma_{inv}(y=y_0) = \sigma_0 \exp(-p_T^2 / 2T_T m). \quad (7)$$

The value of $T_T \approx 116$ MeV for Ar + KCl.

Next, we extend the analysis into a wider region of y . For this purpose we plot

$$\sigma_{inv} / \sigma_{inv}(y=y_0)$$

as a function of p_L/mc in Fig. 4, where p_L is the longitudinal momentum of an emitted proton measured in this "moderate" frame. Data points used here are only for the region of $x \geq 0.5$ (but ≤ 2.0) in Ar + KCl collisions. Over a wide region of x the data points fall on a universal curve of a Gaussian form. This fact implies that σ_{inv} is expressed as

$$\sigma_{inv} = \sigma_0 \exp(-p_T^2/2T_T m) \exp(-p_L^2/2T_L m). \quad (8)$$

For Ar + KCl collisions the best fits were obtained at $T_L \approx 160$ MeV, as shown by a solid curve in Fig. 4. This value of T_L is larger than that of T_T . A dotted curve in Fig. 4 corresponds to the case of $T_L = T_T$, which largely deviates from the data.

Eq. (8) implies that the cross section is factorized as a product of two terms, one which depends only on the transverse momentum (p_T) and the other on the longitudinal momentum (p_L). A similar result has been reported by Antonenko et al.⁸⁾ in their study of proton emission in 3.6 GeV/nucleon α + Pb and C + Pb collisions.

2.2.2. Particle Emission in 'Slow' and 'Fast' Frames

Since the proton spectra at large values of x are reasonably well described by Eq. (8), we assume that particle spectra in both "slow" and "fast" frames are expressed by the same formula but with different values of σ_0 , T_T and T_L . Under this assumption the cross section is expressed by

$$\sigma_{inv} = \sigma_{inv}^{(s)} + \sigma_{inv}^{(m)} + \sigma_{inv}^{(f)}, \quad (9)$$

with

$$\sigma_{inv}^{(i)} = \sigma_0^{(i)} \exp(-p_T^2/2T_T^{(i)} m) \exp(-(p_L^{(i)})^2/2T_L^{(i)} m). \quad (10)$$

Here, $p_L^{(i)}$ is the longitudinal momentum measured in the i^{th} frame, and superscripts $i = s, m$, and f refer to "slow", "moderate", and "fast" frames, respectively.

An example of the decomposition of actual data into the above expression of Eq. (9) is shown in Fig. 5. For deuteron emission in Ar + KCl collisions the parameters for the "moderate" frame were primarily determined from the data at large values of x as well as from the data at around $y = y_0^{(m)} \approx 0.62$, as shown in the left-hand side of Fig. 5. Spectra obtained after the subtraction of $\sigma_{\text{sw}}^{(m)}$ from the data are shown in the right-hand side of Fig. 5. These spectra are very well reproduced with $T_f^{(s)} \approx 82$ MeV and $T_L^{(s)} \approx 56$ MeV. In this case no data are available for obtaining $\sigma_{\text{sw}}^{(f)}$, but, from the symmetry requirement we simply assume that $\sigma_0^{(s)} = \sigma_0^{(f)}$, $T_f^{(s)} = T_f^{(f)}$, and $T_L^{(s)} = T_L^{(f)}$. The final fits to the spectra by Eq. (9) are shown by solid curves in Fig. 2 (as a function of y at various values of x) and also in Fig. 6 (as a function of laboratory momentum at various laboratory angles). Several parameter values obtained from the fits are listed in Table 1. In general, the values of T_T and T_L for the "slow" and "fast" frames are smaller than those for the "moderate" frame. In addition, in the "slow" and "fast" frames we have $T_T \geq T_L$; an opposite tendency to the case of "moderate" frame. It may imply that particles are emitted preferentially in the sideward direction in the "slow" (or "fast") frame, whereas they are emitted more in the forward and backward directions in the "moderate" frame.

2.3. NON-EQUAL-MASS COLLISIONS

We now extend the analysis into the case of non-equal-mass collisions, such as Ne + Pb or Ar + Pb. In this case all the parameters in Eq. (10) as well as the values of $y_0^{(i)}$ ($i = s, m, \text{ and } f$) are free parameters. Therefore, more ambiguities are involved in the analysis, as compared to the case of equal-mass collisions. Nevertheless, we could make a certain fit to the data. As shown in Fig. 7, the data at large values of x mainly determine the value of $y_0^{(m)}$. For Ar + Pb the spectra obtained after the subtraction of $\sigma_{\text{sw}}^{(m)}$ from the data seem to suggest the existence of both "slow" and "fast" frames, as shown in Fig. 8. On the other hand, the present experimental data for Ne + Pb do not require the existence of the "fast" frame. The best fits to the data are shown by solid

curves in Fig. 7, and the fitted parameter values are listed in Table 1.

3. Total Yield and Average Kinetic Energy

3.1. TOTAL PARTICLE YIELDS

By integrating Eq. (10) we can evaluate the total cross section for particle emission in each frame. In the case that $(T_T, T_L) \ll mc^2$ the integration is simply expressed as

$$\sigma_{tot}^{(i)} = (2\pi)^{3/2} T_T (T_L / m_N c^2)^{1/2} (m / m_N)^{1/2} (m_N / c) \sigma_0, \quad (11)$$

where m_N is the nucleon mass. Although the condition of $(T_T, T_L) \ll mc^2$ is not well satisfied in the actual case, the approximation by the above expression is good to within 15 %.

Values of $\sigma_{tot}^{(i)}$ evaluated from Eq. (11) are listed in Table 2. The quantity $R^{(i)}$ listed in this table is the yield relative to the proton yield. We notice the following features:

- (a) Values of $R^{(i)}$ for composite fragments such as d, t, and ^3He are larger for the "slow" and "fast" frames than for the "moderate" frame.
- (b) For nearly equal-mass collisions, the triton to ^3He yield ratio is almost one for the "moderate" frame, whereas it is about two (or more) for the "slow" and "fast" frames.

If we assume that each frame corresponds to a certain source like a fireball, then T_T or T_L roughly corresponds to the "temperature" of the source. Then the composite fragments are more easily created in the fireball at lower temperature. Within the framework of thermal or statistical models, therefore, the observation (a) seems consistent with the observed fact that the value of T is larger for the "moderate" frame than for the "slow" (or "fast") frame. With regard to the observation (b), the data may indicate the importance of Coulomb effects for the "slow" and "fast" frames.

3.2. AVERAGE KINETIC ENERGY OF PARTICLES FROM EACH FRAME

By using Eq. (10) we can also evaluate an average kinetic energy, $\langle W \rangle$, of emitted particles. In the limit of $(T_T, T_L) \ll mc^2$ we have

$$\langle W \rangle^{(i)} \approx T_T^{(i)} + T_L^{(i)} / 2, \quad (12)$$

where $\langle W \rangle^{(i)}$ is the average kinetic energy of emitted particles in the i^{th} frame. The calculated values of $\langle W \rangle^{(i)}$ are listed in Table 3. Once the type of frame is fixed, the average kinetic energy in this frame is almost independent of the mass of emitted particles. Also, it does not strongly depend on the projectile and target masses. A significant feature observed in Table 3 is that the value of $\langle W \rangle^{(i)}$ for the "moderate" frame is a factor of two larger than the corresponding values for the "slow" and "fast" frame; about 200 MeV in the former case and 100 MeV in the latter. Also, we must notice that the value of $\langle W \rangle^{(i)}$ for the "slow" or "fast" frame is a factor of 10 larger than the average nucleon binding energy (≈ 8 MeV).

4. Comparison with Participant-Spectator Model

So far, we have not reached any clear understanding of the nature of each frame and the mechanism of its formation. In terms of the participant-spectator model⁴⁻⁷, one might guess that the "slow" and "fast" frames correspond to the spectator region while the "moderate" frame to the participant. However, there are a number of difficulties in making such correspondences. For example, the values of $y_0^{(s)}$ and $y_0^{(f)}$ are too far from values of the target rapidity $y_T (= 0)$ and the projectile rapidity $y_P (= 1.23)$, respectively. In addition, the average kinetic energy, $\langle W \rangle^{(i)}$, for the "slow" or "fast" frame is too large compared to the value expected for the spectator region; we expect $\langle W \rangle^{(i)} \approx 12$ MeV for this region. In this section we first describe the traditional participant-spectator model and point out a certain difficulty found in this model. Then, we describe a possible interpretation for the present results.

4.1. A PUZZLE IN THE PARTICIPANT-SPECTATOR MODEL

Suppose that the projectile nucleus consists of Z_P protons and N_P neutrons (and therefore, $A_P = Z_P + N_P$). Similarly, suppose that the target nucleus consists of A_T nucleons. Then, the traditional participant-spectator model (in which straight-line trajectories are assumed) gives the following formulas for the total integrated yield of nuclear charge⁷⁾:

$$\sigma_{tot}^{charge} = Z_{eff} \cdot \pi r_0^2 (A_P^{1/3} + A_T^{1/3})^2, \quad (13)$$

where

$$Z_{eff} = \frac{Z_P A_T^{2/3} + Z_T A_P^{2/3}}{(A_P^{1/3} + A_T^{1/3})^2} \quad \text{for participant,} \quad (14a)$$

$$Z_{eff} = Z_P \frac{A_T^{2/3} + 2A_P^{1/3}A_T^{1/3}}{(A_P^{1/3} + A_T^{1/3})^2} \quad \text{for projectile spectator,} \quad (14b)$$

$$Z_{eff} = Z_T \frac{A_P^{2/3} + 2A_P^{1/3}A_T^{1/3}}{(A_P^{1/3} + A_T^{1/3})^2} \quad \text{for target spectator.} \quad (14c)$$

Here, the value of r_0 is typically 1.0-1.2 fm.

In refs.^{7,2,9)} these formulas are compared with data. The observed projectile- and target-mass dependences are reproduced very well by these formulas. With regard to the absolute cross sections, however, Eq. (13) with $r_0 = 1.2$ fm overestimates the yield for both projectile and target fragments (by 30-40 %) as compared to the data, whereas it explains reasonably well the data at large angles (which are primarily related to the participant region). Empirically, the available data of total nuclear charge can be explained with $r_0 = 0.95$ fm for projectile fragments and with $r_0 = 1.20$ fm for the data at large angles⁹⁾.

Why should we use a somewhat smaller value of r_0 for projectile fragments? Obviously the participant-spectator model is based on an extreme simplification. Some nucleons involved in a collision might be classified neither as participant nor as spectator. These nucleons may exhibit a nature intermediate between the participant and spectator. In the analysis reported in refs.^{7,2,9)} these intermediate nucleons are

more likely counted in the data at large angles but not in the data of projectile fragments. This might be the reason why the data at large angles require a larger value of r_0 while the data of projectile and target fragments require a smaller value of it.

4.2. A POSSIBLE EXPLANATION FOR THE PRESENT RESULTS

The present analysis suggests that perhaps three well-clustered sources may exist, one located at around half the projectile rapidity and the other two located close to y_T and y_P . We thus assume that five sources are created in a nuclear collision, the target-spectator, hot-target, participant, hot-projectile, and projectile-spectator sources. Experimentally the first and last sources have been rather well established¹⁰⁻¹²); they are located almost exactly at $y = y_T$ and y_P and can be classified as spectator. The hot-target and hot-projectile sources are completely new that have never been proposed so far. These correspond to the "slow" and "fast" frames, respectively, in the present analysis, and the participant source corresponds to the "moderate" frame.

In the mid-rapidity region the fireball model⁵) predicts a single source located at the rapidity of the effective c.m. frame of the fireball, while the firestreak model¹³) as well as the row-on-on cascade model⁶) predicts a string-like continuous source whose rapidity ranges widely from y_T to y_P . No theories have predicted three well-clustered sources in this region. Perhaps the hot-target and hot-projectile sources proposed here may only be able to relate to the intermediate nucleons which belong neither to participant nor to spectator, as mentioned in the previous section.

In connection with this hot-projectile source we cite a recent work by Baumgardt et al.¹⁴) in which p_T distributions of α particles have been measured at $y \approx y_P$ in collisions of 1.9 GeV/nucleon Fe + emulsion. They demonstrated that two classes of events might exist, one associated with a cold source with temperature $T \approx 10$ MeV and the other associated with a moderately hot source with $T \approx 40$ MeV. The present hot-

projectile source may correspond to this moderately hot source.

Under the assumption that five sources exist, we show in Table 4 the nuclear charge distributions over several sources. Values of nuclear charge for the projectile-spectator and target-spectator sources were evaluated from the systematics reported in refs.^{7,9}). Values for the other three sources are based on the present analysis. The parameter τ_0 was chosen to $\tau_0 = 1.07$ fm so that the sum of nuclear charges, $\sum Z_{eff}^{(i)}$, for five sources yields approximately the total nuclear charge, $Z_P + Z_T$. For nearly equal-mass collisions nuclear charges are distributed almost equally over the target-spectator source, participant source, and the projectile-spectator source. The hot-target and hot-projectile sources carry much less charges than these three. The value of nuclear charge involved in the participant source is almost equal to Z_{eff} evaluated from Eq. (14a), while that involved in the projectile-spectator source is about 2/3 of that expected from Eq. (14b).

Of course, the above statement of five sources is largely based on our guess, and obviously more detailed studies over a much wider kinematical region of fragments as well as at other beam energies and with other projectile and target mass combinations are required to pin down this five-source question.

5. Summary

The present kinematical analysis revealed the following features:

- (a) Fragment emission at large angles can be decomposed into three contributions from "slow", "moderate" and "fast" moving frames. For nearly equal-mass collisions, the rapidities of these frames are 0.22, 0.62 and 1.02 at the beam energy of 800 MeV. Note that in this case the target and projectile rapidities are 0 and 1.23, respectively.
- (b) Fragment spectra in each frame can be factorized as a product of two Gaussian-type distributions, one which involves only p_T and the other which involves only p_L .

where p_L is the longitudinal momentum measured in that frame.

- (c) Widths of Gaussian distributions, characterized by T_T and T_L , have features such that $T_T \geq T_L$ for the "slow" and "fast" frames while $T_T \leq T_L$ for the "moderate" frame. This implies that the sideward particle emission is favored in the "slow" and "fast" frames while the forward-backward emission is favored in the "moderate" frame.
- (d) Composite fragment emission is more favored in the "slow" (or "fast") frame than in the "moderate" frame. In addition, the $t/{}^3\text{He}$ ratio reaches about two in the former case while it is almost one in the latter.
- (e) If these three frames correspond to certain sources, then the "slow" and "fast" sources may be attributable to nucleon groups which belong neither to participant nor to spectator. These two sources cannot be explained by the traditional participant-spectator model.

Unfortunately, no currently available theories can interpret the above features, except perhaps the point (d). Further extended analysis and theoretical studies are now under progress.

We would like to express our sincere thanks to K. V. Karadjev and M. S. Ippolitov for their help during several stages of the analysis. Useful discussions with H. Gutbrod, M. Gyulassy, G. Shapiro, I. N. Mishustin, V. M. Galitskii and S. T. Belajev are gratefully acknowledged. One of the authors (V.I.M.) would like to express his deep gratitude to the staff at Lawrence Berkeley Laboratory for their warm hospitality during his stay there. This work was supported by the Director, Office of Energy Research, Division of Nuclear Physics of the Office of High Energy and Nuclear Physics of the U.S. Department of Energy Contract DE-AC03-76SF00098. It was also supported by the INS-LBL Collaboration Program.

References

- 1) Recent progresses of both experimental and theoretical studies are summarized, for example, in Proceedings of Fifth High Energy Heavy Ion Summer Study, Berkeley, May, 1981, edited by L. S. Schroeder, Lawrence Berkeley Laboratory Report LBL-12652 UC-34 CONF-8105104.
- 2) S. Nagamiya, M.-C. Lemaire, E. Moeller, S. Schnetzer, G. Shapiro, H. Steiner, and I. Tanihata, Phys. Rev. **C24** (1981) 971.
- 3) M.-C. Lemaire, S. Nagamiya, O. Chamberlain, G. Shapiro, S. Schnetzer, H. Steiner, and I. Tanihata, Lawrence Berkeley Laboratory Report LBL-8463 (1979), unpublished.
- 4) J. D. Bowman, W. J. Swiatecki, and C. F. Tsang, Lawrence Berkeley Laboratory Report LBL-2908 (1973), unpublished.
- 5) G. D. Westfall, J. Gosset, P. J. Johansen, A. M. Poskanzer, W. G. Meyer, H. H. Gutbrod, A. Sandoval, and R. Stock, Phys. Rev. Lett. **37** (1976) 1202.
- 6) J. Hufner and J. Knoll, Nucl. Phys. **A290** (1977) 460.
- 7) S. Nagamiya, Nucl. Phys. **A335** (1980) 517.
- 8) V. G. Antonenko, V. M. Galitskii, Yu. I. Grigor'yan, M. S. Ippolitov, K. V. Karadjev, E. A. Kuz'min, V. I. Manko, A. A. Ogloblin, V. V. Paramonov, A. A. Tsvetkov, and A. A. Vinogradov, Institute of Atomic Energy Preprint, IAE-3220 (1979).
- 9) S. Nagamiya, Proceedings of the Fifth High Energy Heavy Ion Summer Study, Berkeley, May, 1981, edited by L. S. Schroeder, LBL-12652 UC-34 CONF-8105104, p. 141.
- 10) D. E. Greiner, P. J. Lindstrom, H. Heckman, B. Cork, and F. S. Bieser, Phys. Rev. Lett. **35** (1975) 152.
- 11) L. Anderson, Thesis, Lawrence Berkeley Laboratory Report LBL-6767 (1977), unpublished.
- 12) D. J. Morrissey, W. Loveland, M. de Saint Simon and G. T. Seaborg, Phys. Rev. **C21**

(1980) 1783.

13) W. D. Myers, Nucl. Phys. **A296** (1978) 177.

14) H. G. Baumgardt, E. M. Friedlander and E. Schopper, J. Phys. **G7** (1981) L175.

Table 1
Fitted values of various parameters

Reaction Fragment		"Slow" Frame				"Moderate" Frame				"Fast" Frame			
		γ_0	$\sigma_0^a)$	T_T (MeV)	T_L (MeV)	γ_0	$\sigma_0^a)$	T_T (MeV)	T_L (MeV)	γ_0	$\sigma_0^a)$	T_T (MeV)	T_L (MeV)
Ne+NaF	p	0.22	3450	75	51	0.62	8100	105	145	1.02	3450	75	51
	d	"	950	83	56	"	900	105	145	"	950	83	56
	t	"	170	83	56	"	69	105	145	"	170	83	56
	^3He	"	50	90	61	"	50	120	165	"	50	90	61
<hr/>													
Ar+Kcl	p	0.22	8000	77	53	0.62	20500	116	160	1.02	8000	77	53
	d	"	2540	82	56	"	2240	134	185	"	2540	82	56
	t	"	426	89	61	"	186	136	189	"	426	89	61
	^3He	"	200	94	64	"	200	144	199	"	200	94	64
<hr/>													
Ne+Pb	p	0.13	60000	60	40	0.47	35000	115	150				
	d	"	15200	70	47	"	6300	117	153				
	t	"	5900	80	50	"	770	120	155				
<hr/>													
Ar+Pb	p	0.20	54000	73	50	0.51	45000	127	160	1.05	8400	95	60
	d	"	19000	85	58	"	6600	145	182	"	2800	95	60
	t	"	7200	85	58	"	900	145	182	"	500	95	60

a) In units of $(\text{GeV}\cdot\text{mb}/\text{sr})/(\text{GeV}/c)^3$.

Table 2
Total particle yields from each frame

Reaction Fragment		"Slow" Frame σ_{tot} R ^{a)} (barn)		"Moderate" Frame σ_{tot} R ^{a)} (barn)		"Fast" Frame σ_{tot} R ^{a)} (barn)		$\sigma_{\text{tot}}^{(s)} : \sigma_{\text{tot}}^{(m)} : \sigma_{\text{tot}}^{(f)}$
Ne+NaF	p	0.89	1	4.96	1	0.89	1	1:5.5:1
	d	0.40	0.45	0.78	0.16	0.40	0.45	1:1.9:1
	t	0.089	0.10	0.073	0.015	0.089	0.10	1:0.82:1
	³ He	0.030	0.033	0.065	0.013	0.030	0.033	1:2.2:1
	Total ^{b)}	1.44	1.62	5.94	1.20	1.44	1.62	1:4.1:1

Ar+KcI	p	2.17	1	14.55	1	2.17	1	1:6.7:1
	d	1.07	0.49	2.8	0.19	1.07	0.49	1:2.6:1
	t	0.25	0.11	0.29	0.020	0.25	0.11	1:1.2:1
	³ He	0.13	0.058	0.34	0.023	0.13	0.058	1:2.7:1
	Total ^{b)}	3.75	1.73	18.3	1.26	3.75	1.73	1:4.9:1

Ne+Pb	p	11	1	24	1			1:2.2
	d	5	0.45	3.6	0.15			1:0.71
	t	2.8	0.25	0.68	0.028			1:0.24
	Total ^{b)}	18.8	1.71	28.3	1.18			1:1.5

Ar+Pb	p	13.5	1	35	1	3	1	1:2.6:0.22
	d	8.4	0.62	8.8	0.25	1.4	0.47	1:1.05:0.17
	t	3.9	0.29	1.5	0.042	0.31	0.10	1:0.38:0.08
	Total ^{b)}	25.8	1.91	45.3	1.29	4.71	1.57	1:1.8:0.18

a) R is defined by $\sigma_{\text{tot}}(\text{fragment})/\sigma_{\text{tot}}(\text{Proton})$.

b) Total nuclear Charge.

Table 3
Average kinetic energy of particles from each frame.

Reaction	Fragment	$\langle W \rangle^{(s)}$ (MeV)	$\langle W \rangle^{(m)}$ (MeV)	$\langle W \rangle^{(f)}$ (MeV)
Ne+NaF	p	100	177	100
	d	111	177	111
	t	111	177	111
	^3He	120	202	120

Ar+KCl	p	103	196	103
	d	110	226	110
	t	119	231	119
	^3He	126	244	126

Ne+Pb	p	80	190	
	d	93	193	
	t	105	197	

Ar+Pb	p	98	207	125
	d	114	236	125
	t	114	236	125

Table 4
Distribution of nuclear charges over several sources

Reaction	$\sigma_{\text{geom}}^{\text{a)}$ (barn)	Z_{eff}					Sum of Z_{eff}	$Z_{\text{p}} + Z_{\text{T}}$
		Target- Spectator Source	Hot- Target Source	Participant Source	Hot- Projectile Source	Projectile- Spectator Source		
Ne+NaF	1.08	5.9 ^{b)}	1.3	5.5	1.3	5.9 ^{b)}	19.9	20
Ar+KCl	1.64	11.4 ^{b)}	2.3	11.1	2.3	11.4 ^{b)}	38.5	38
Ne+Pb	2.68	71.2 ^{b)}	7.0	10.6	---	4.2 ^{b)}	93.0	92
Ar+Pb	3.13	68.3 ^{b)}	8.2	14.5	1.5	8.5 ^{b)}	101.0	100

a) $\sigma_{\text{geom}} \equiv \pi r_0^2 (A_p^{1/3} + A_T^{1/3})^2$ with $r_0 = 1.07$ fm.

b) Values obtained from the data systematics reported in Refs.^{7,9)}.

FIGURE CAPTIONS

Fig. 1 Lorentz-invariant cross sections plotted as a function of y for various values of x , in the case of a Boltzmann-type distribution in the nucleon-nucleon c.m. frame at $E_{beam}^{lab}/A = 800$ MeV.

Fig. 2 Experimental data for production of p, d, t, and ^3He in 800 MeV/nucleon Ar + KCl and Ne + NaF collisions. Data are taken from refs.^{2,3}.

Fig. 3 Invariant cross sections, σ_{inv} , for protons plotted as a function of the transverse energy (left) and the squares of the transverse momentum (right).

Fig. 4 Ratios $\sigma_{inv}/\sigma_{inv}(y=y_0)$ plotted as a function of p_L/mc , where p_L is the longitudinal momentum of emitted proton measured in the frame whose rapidity is y_0 . Data are shown only for x [defined by Eq. (4)] ≥ 0.5 in Ar + KCl collisions.

Fig. 5 An example of the data decomposition into three frames in deuteron emission in Ar + KCl collisions. Only "slow" and "moderate" frames are required to fit these data.

Fig. 6 Example of the fits to the actual laboratory spectra.

Fig. 7 Experimental data for production of p, d, t, and ^3He in 800 MeV/nucleon Ar + Pb and Ne + Pb collisions. Data are taken from refs.^{2,3}.

Fig. 8 An example of the data decomposition into three frames in proton emission in Ar + Pb collisions.

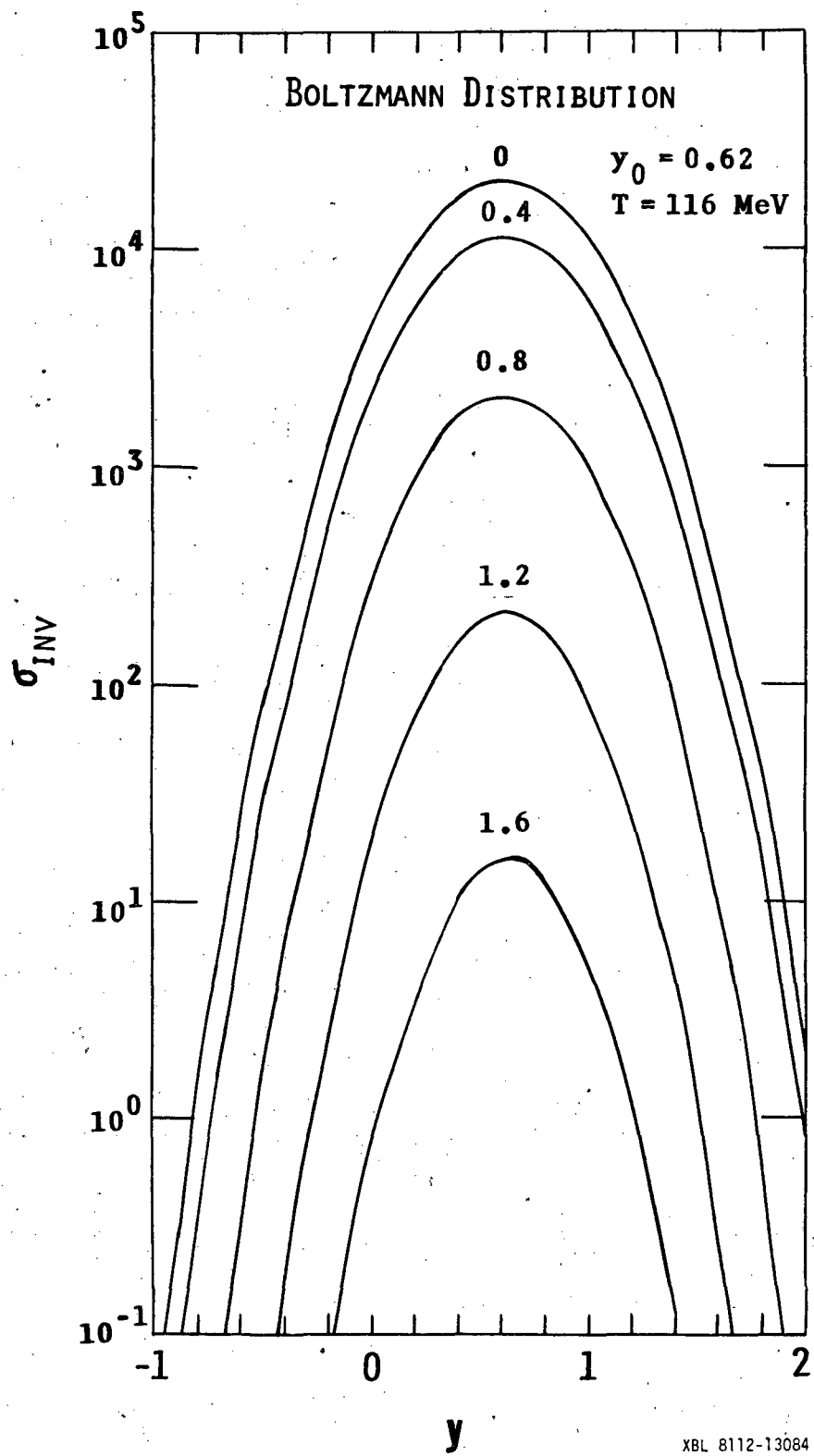


Fig. 1

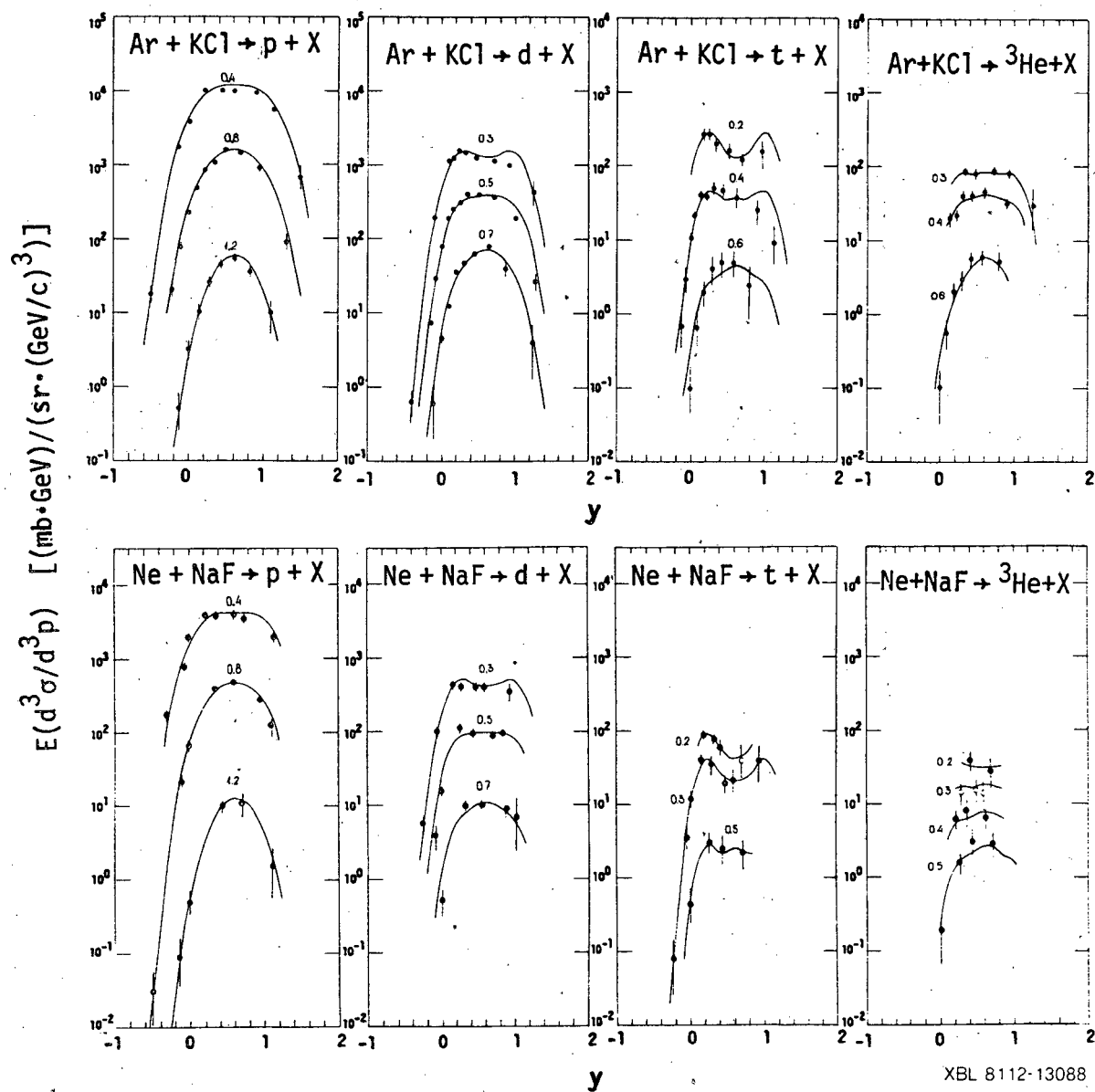
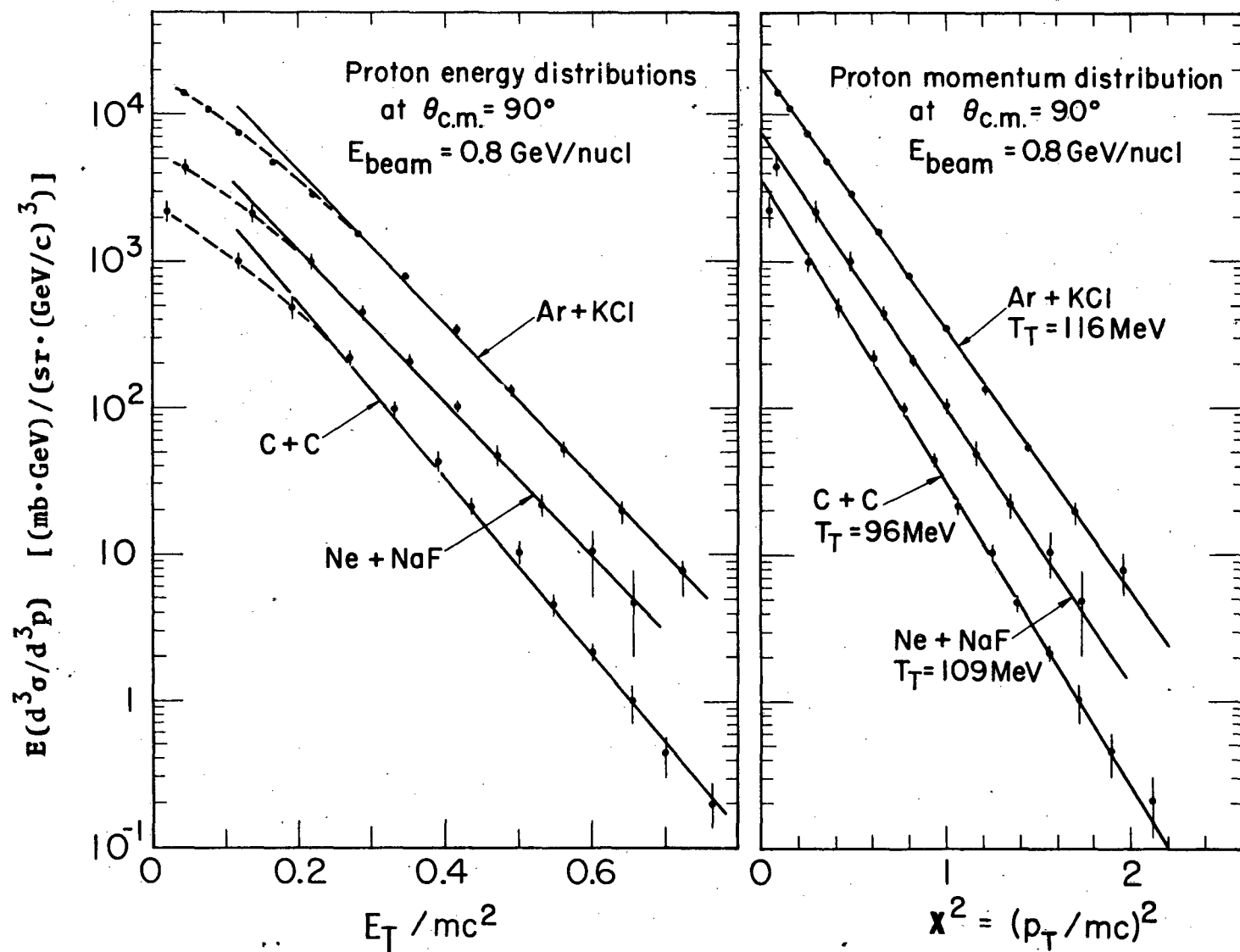


Fig. 2



XBL7912-3942

Fig. 3

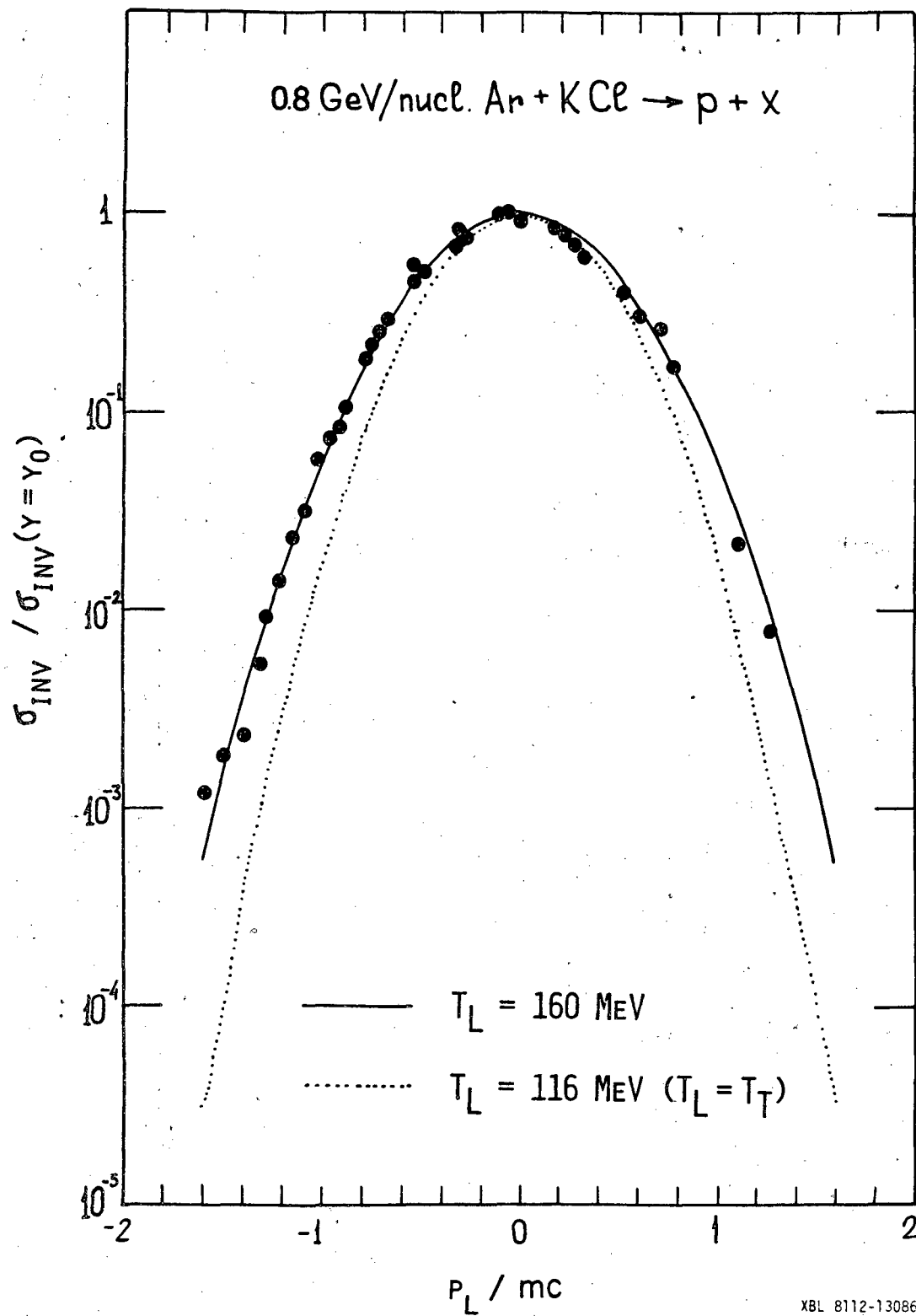
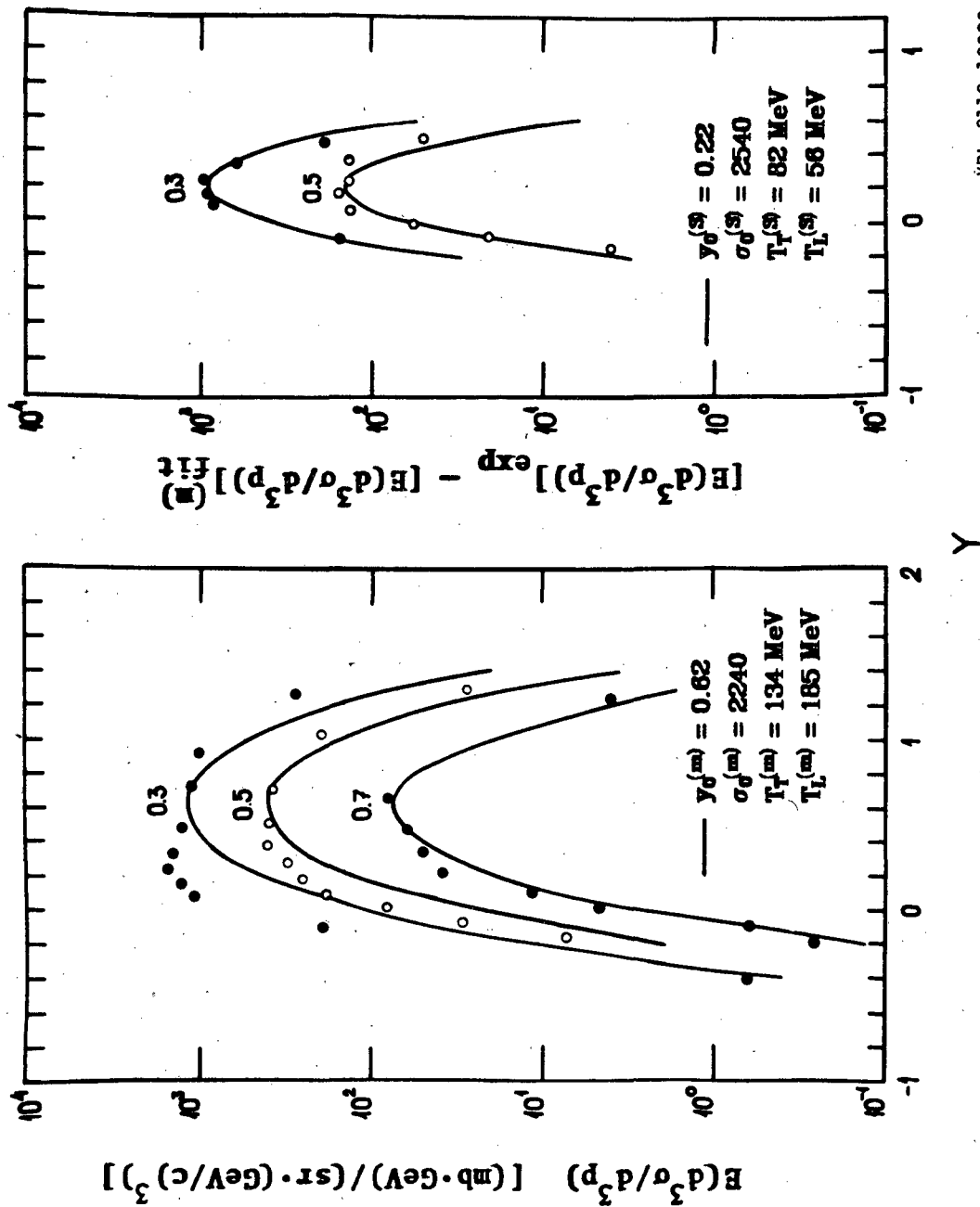


Fig. 4

0.8 GeV/nucleon Ar + KCl \rightarrow d + X



XBL 8112-13083

Fig. 5

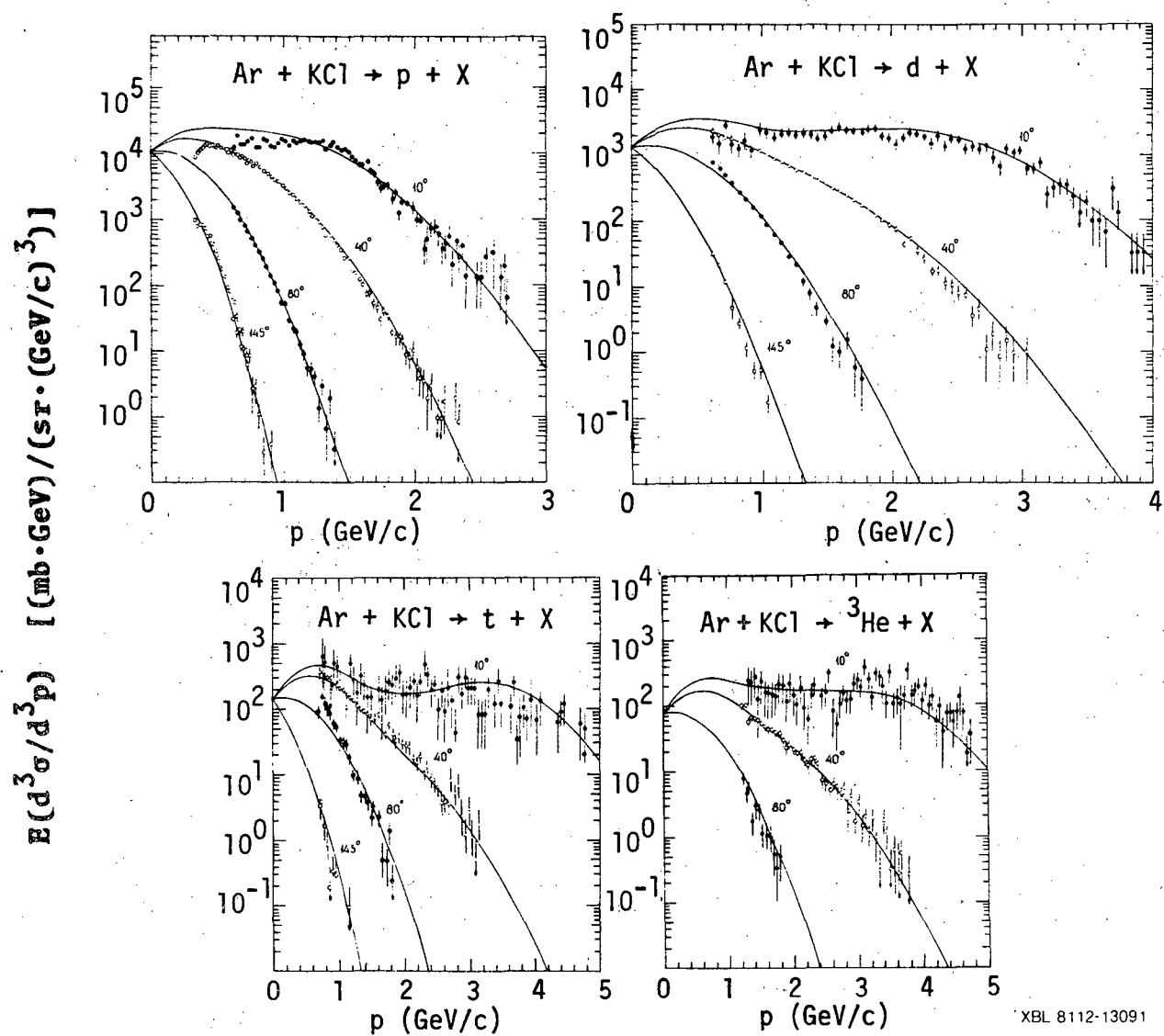
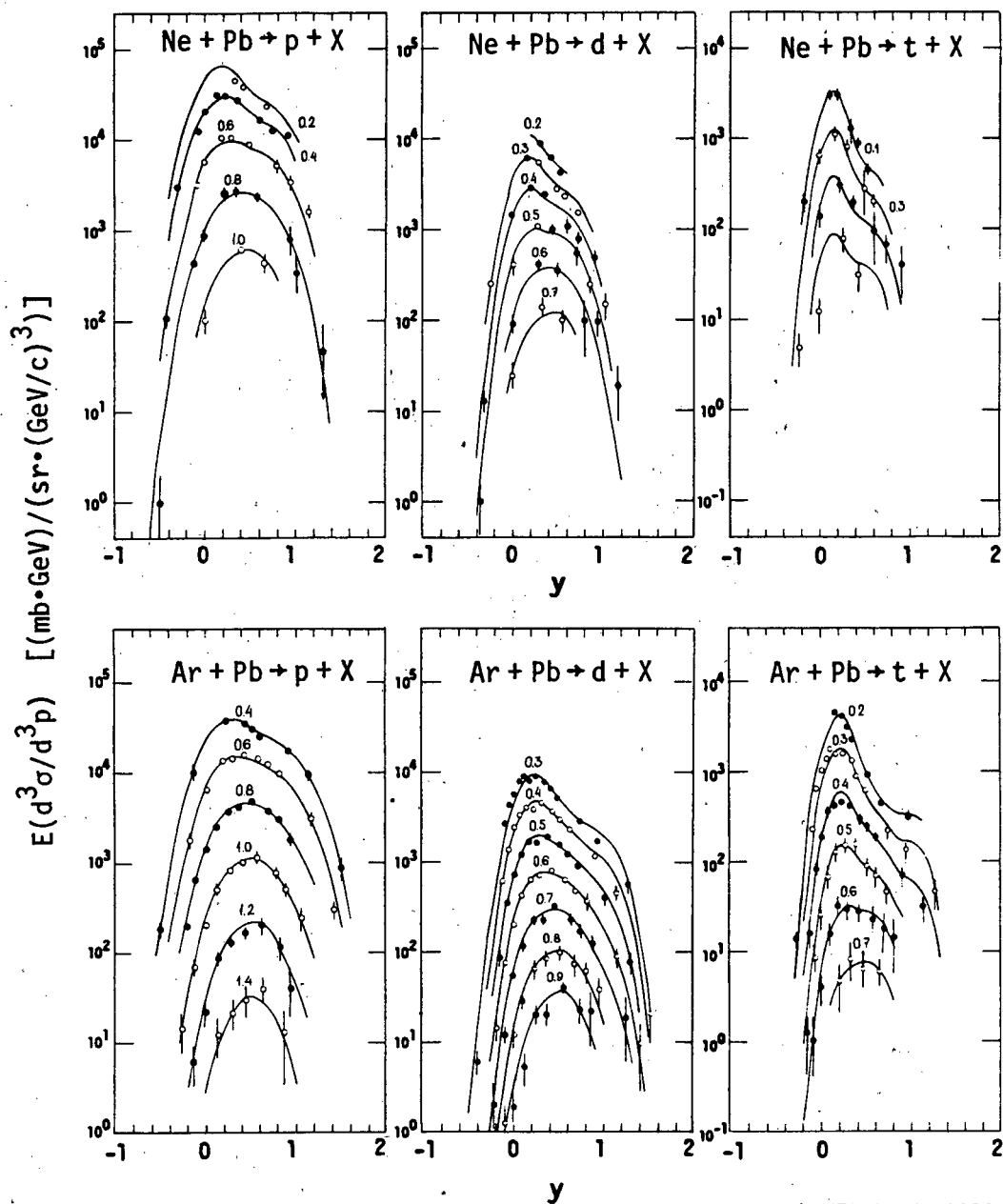


Fig. 6



XBL 8112-13090

Fig. 7

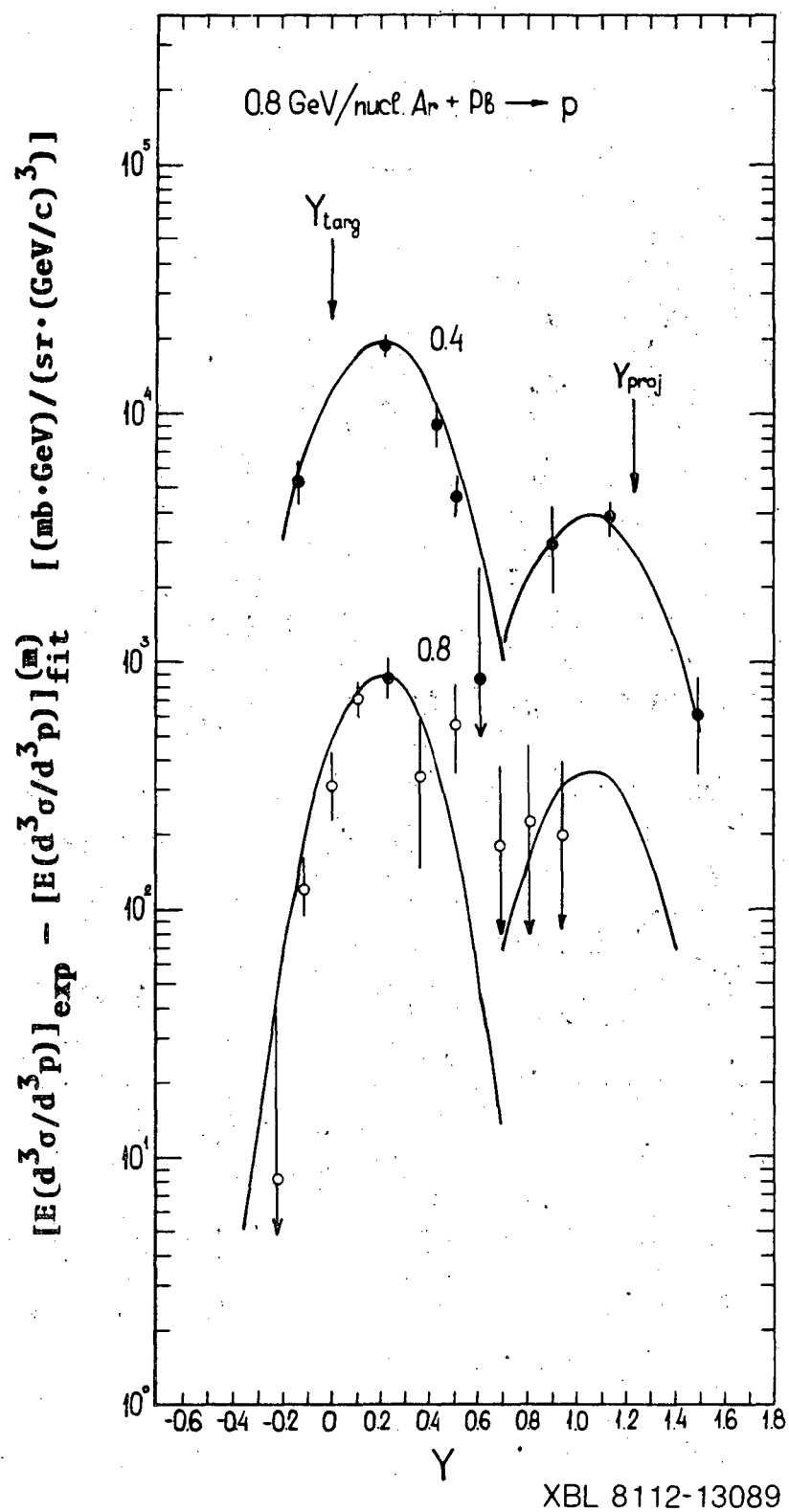


Fig. 8

This report was done with support from the Department of Energy. Any conclusions or opinions expressed in this report represent solely those of the author(s) and not necessarily those of The Regents of the University of California, the Lawrence Berkeley Laboratory or the Department of Energy.

Reference to a company or product name does not imply approval or recommendation of the product by the University of California or the U.S. Department of Energy to the exclusion of others that may be suitable.

TECHNICAL INFORMATION DEPARTMENT
LAWRENCE BERKELEY LABORATORY
UNIVERSITY OF CALIFORNIA
BERKELEY, CALIFORNIA 94720